Supporting Information for:

Patchiness of plankton communities at fronts explained by Lagrangian history of upwelled water parcels

Shailja Gangrade[1*] and Inès Mangolte[2,3]

[1]Scripps Institution of Oceanography, University of California San Diego, La Jolla, California, USA

[2]LOCEAN (Laboratoire d'Océanographie et du Climat), Institut Pierre Simon Laplace (Sorbonne Université/CNRS/IRD/MNHN), Paris, France

[3]ENTROPIE, IRD/Université de la Réunion/Université de Nouvelle-Calédonie/CNRS/Ifremer, Noumea, New Caledonia

[*]Corresponding author: Shailja Gangrade, sgangrad@ucsd.edu

Biological responses of non-diatom and non-copepod taxa

The diatom-copepod food chain, despite its importance (both in terms of quantity and in ecological and biogeochemical consequences), is one dimension of a very complex plankton ecosystem. On the one hand, many other grazing zooplankton taxa also consume diatoms (particularly filter-feeding tunicates); on the other hand, the diet of copepods can include a variety of sources including other phytoplankton, zooplankton, or detritus (Whitmore and Ohman, 2021).

Many factors might explain why the collected data only showed a significant biological response for diatoms and copepods. In the case of non-diatom phytoplankton (Figure S6), it is possible that a bloom developed at the subsurface only and was thus not measured in our surface measurements. Or, it is also possible that – unlike diatoms – the other phytoplankton taxa were unable to escape grazing pressure due to their slower growth rates (Inomura et al., 2023). In the case of carnivorous zooplankton (Figure S7), it is likely that the duration of our backtracking analysis (two months) was too short relative to their reproduction rates. We would expect large changes in their abundances to be visible after several months or even years. For instance, Messié et al. (2023) described a "damping effect" in the California upwelling region by which metazoan organisms with longer lifespans or those located deeper in the water column (i.e., mesopelagic or benthic) respond slower to environmental forcings than phytoplankton or micro-zooplankton: the response time scales may be months to years as opposed to days to weeks.

Moreover, some taxa showed multiple peaks in abundance within water parcels of different ages, which could indicate more complex trophic interactions. For instance, appendicularians (Figure S8a) showed an initial peak at about 10 days, consistent with their fast growth rate in response to the diatom bloom (Capitanio and Esnal, 1998), followed by a second peak at about 30 days, which could be generated by the consumption of copepod fecal pellets.

The only taxon other than diatoms and copepods that showed a clear relationship with age since upwelling pulse was rhizarians. The abundance of rhizarians peaked at approximately 30 days (Figure S8b). While the feeding strategies and growth rates of rhizarian organisms are extremely diverse (Biard, 2015; Biard and Ohman, 2020), the time scale of this increase in abundance is consistent with a growth response to an increase in the availability of their nutrition source (whether they are photosynthetic, eat inorganic nutrients, diatoms, or detritus).

Table S1. List of plankton taxa sampled during the E-Front transects, the methodologies used (sampling and identification methods), and the vertical resolution.

Sample	Instrument	Taxa included	Depth
Niskin bottle	Flow Cytometry	Heterotrophic bacteria, *Prochlorococcus* (PRO), *Synechococcus* (SYN), pico-eukaryotes	Discrete levels 0-120 m
Niskin bottle	HPLC	Diatoms, dinoflagellates, coccolithophores, pelagophytes, chlorophytes, cryptophytes	Surface
Bongo net	ZooScan	3 copepod groups (calanoids, oithonoids, and others), pteropods, euphausiids, other crustaceans, rhizarians, doliolids, appendicularians, salps, pyrosomes, cnidarians+ctenophores, polychaetes, chaetognaths, ostracods	Vertically averaged 0-100 m

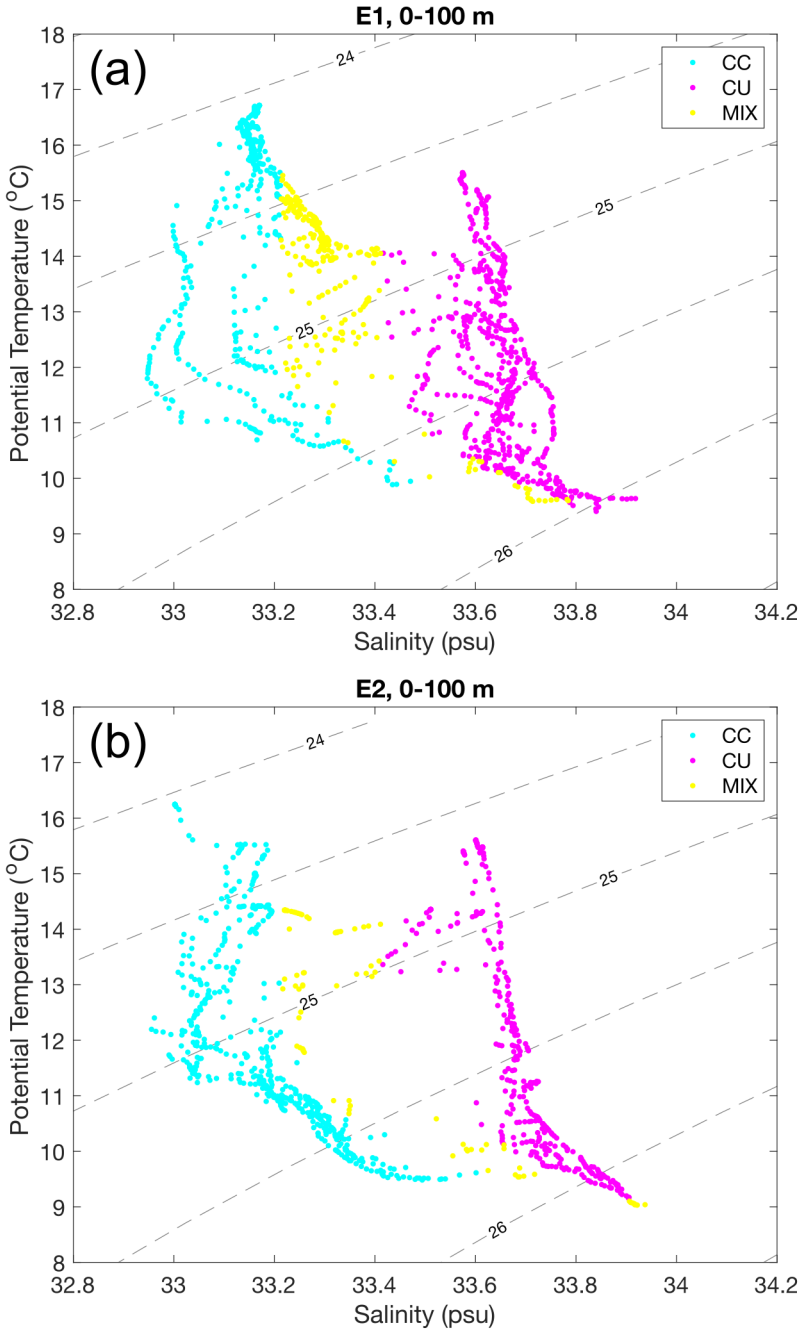

Figure S1. Salinity-temperature plots for E-Front Transect E1 (a) and Transect E2 (b) from CTD vertical profiles (0-100 m). Dashed gray lines indicate the density (σ_θ) isolines. Points are colored according to their water-mass type classification: California Current (CC, cyan), California Undercurrent (CU, magenta) and MIX (yellow).

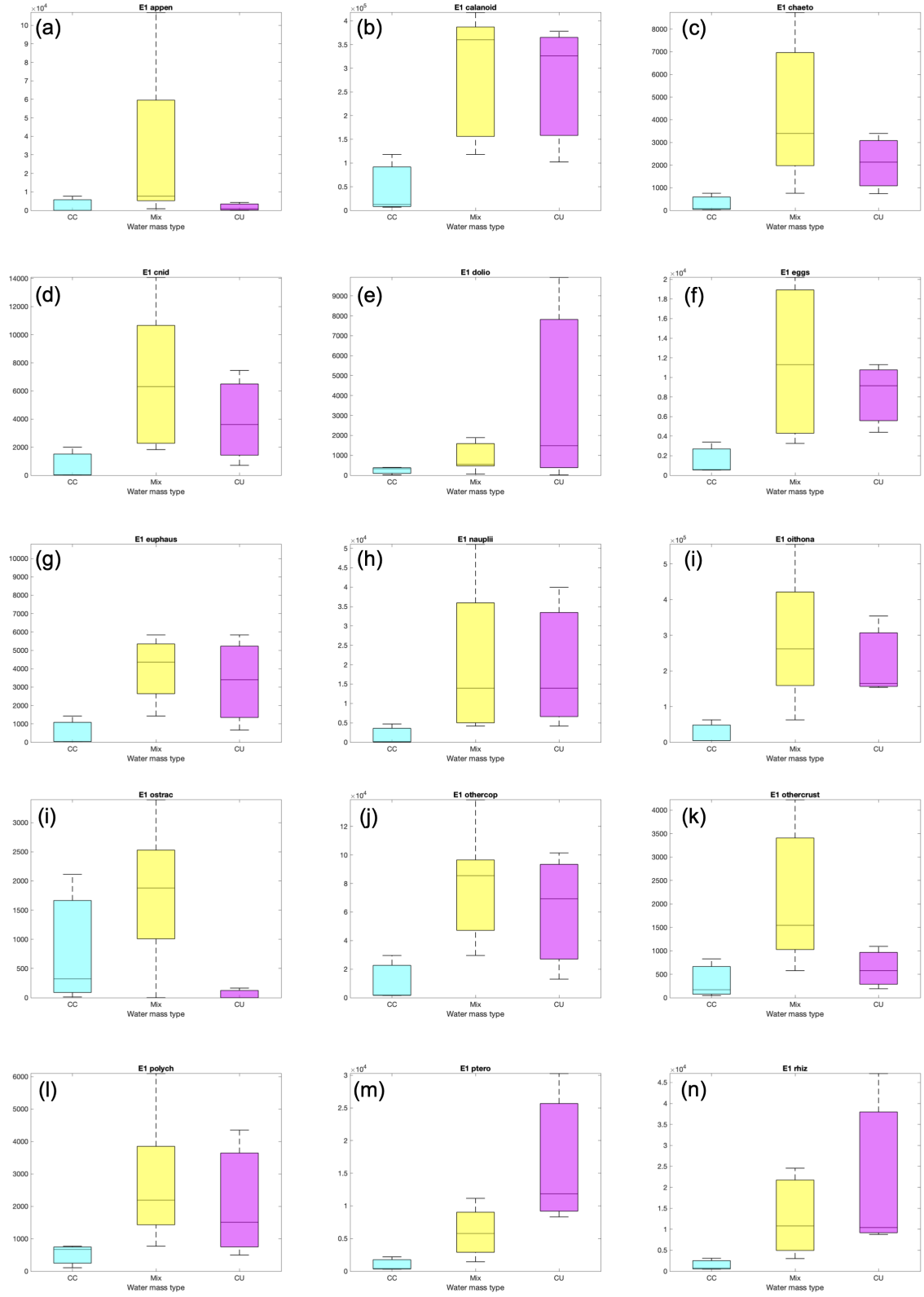

Figure S2. Distribution of zooplankton abundance ($no./m^2$) in each majority water-mass type for E-front Transect E1. Box plots indicate the median and interquartile ranges of abundance and are colored by the corresponding water-mass type (cyan for CC, yellow for MIX, and magenta for CU). Zooplankton abundances were vertically integrated (0-100m), and the majority water-mass type in the vertical water-column profile was used (see Data and Methods).

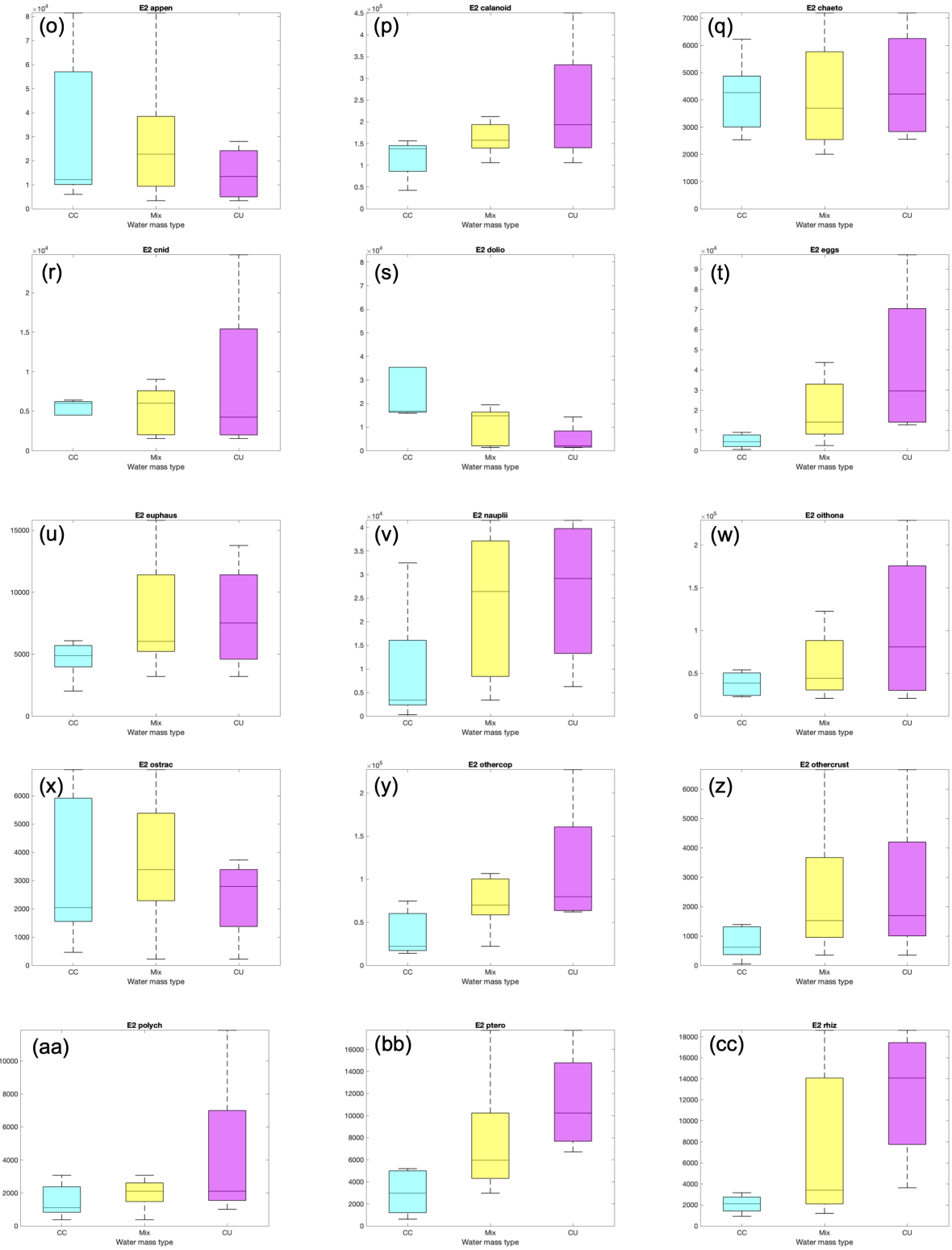

Figure S3. Same as Figure S2 above, but for E-Front Transect E2.

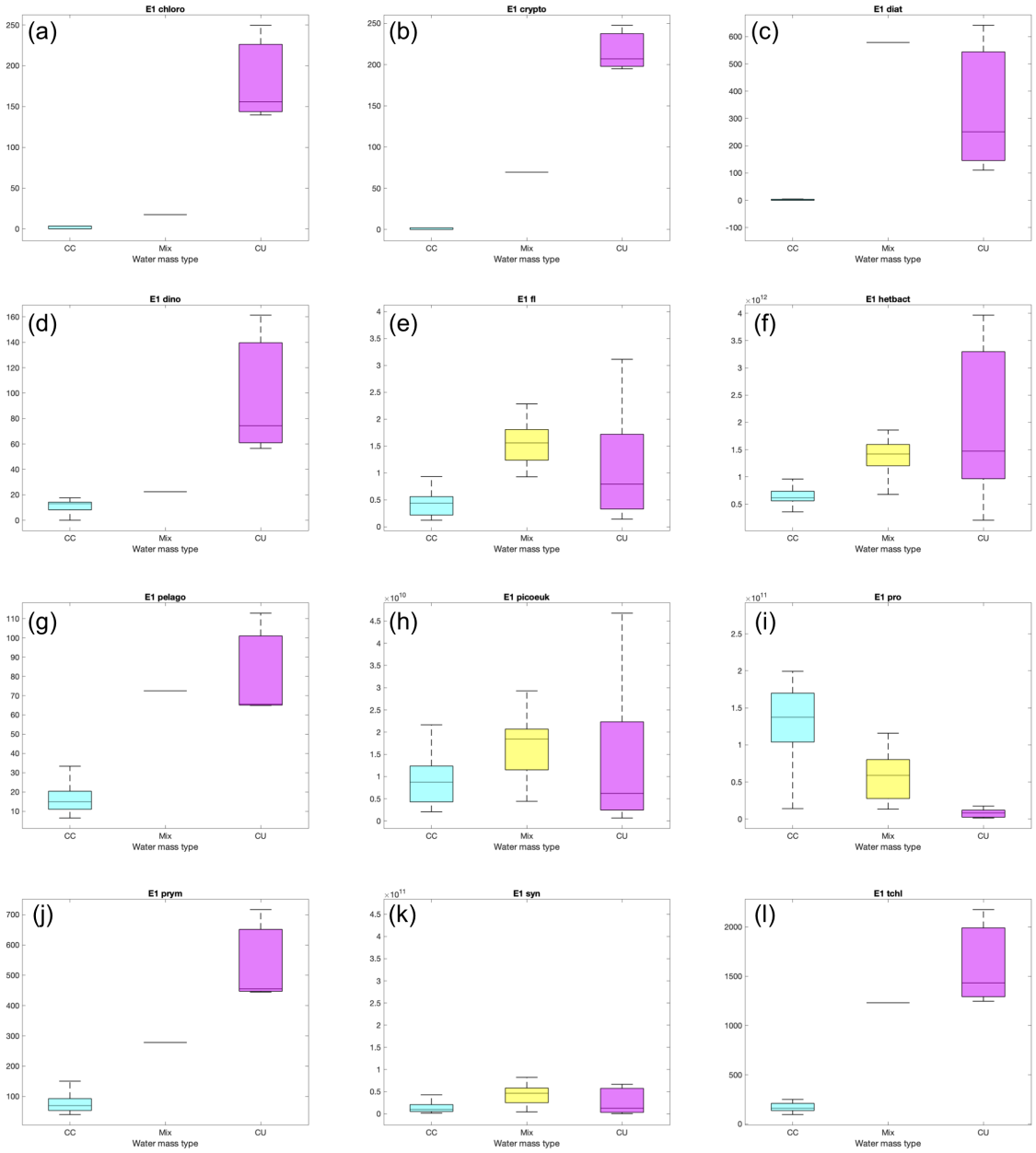

Figure S4. Distribution of picoplankton and phytoplankton abundance in each majority water-mass type for E-Front Transect E1. Box plots indicate the median and interquartile ranges of abundance and are colored by corresponding water-mass type (cyan for CC, yellow for MIX, and magenta for CU). Picoplankton abundance (*Prochlorococcus*, *Synechococcus*, picoeukaryotes, and heterotrophic bacteria, in $cells/L$) were measured with flow cytometry at each vertical level. Phytoplankton ($\mu gChl/m^3$) were measured with HPLC for the surface sample only. The water-mass types were taken at the vertical level corresponding to each sample.

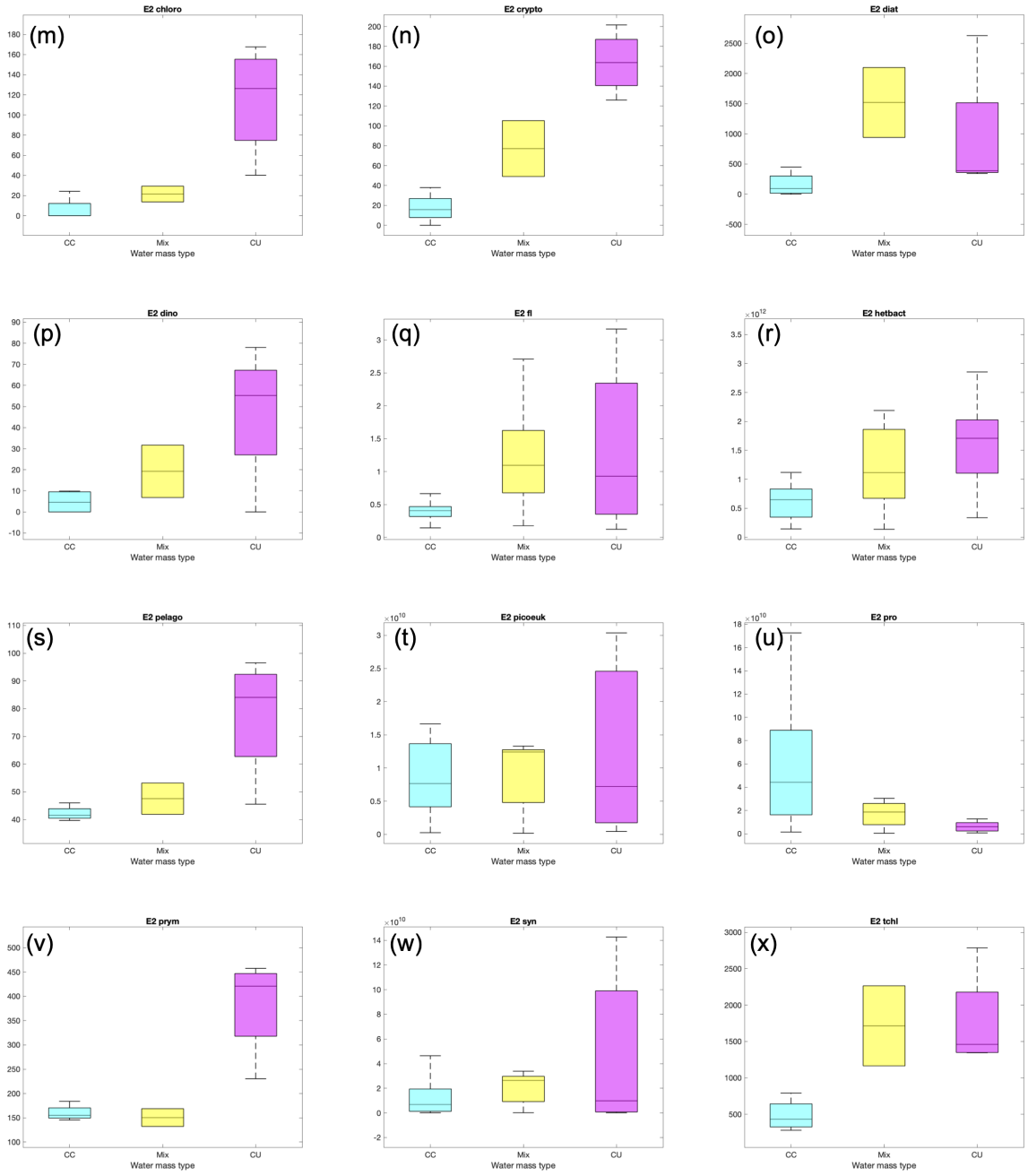

Figure S5. Same as Figure S4 above, but for E-Front Transect E2.

Table S2. Results from Kruskal-Wallis statistical tests comparing the distributions of plankton abundances in pairs of water-mass types (CC vs. CU, CC vs. MIX and CC vs. MIX) for E-Front Transect E1. High p-values (> 0.05) indicate that the distributions are not statistically different (i.e., the null hypothesis – that the data originate from the same distributions – is not rejected). In contrast, low p-values ≤ 0.01 (orange) and $0.01 < p$-value < 0.05 (yellow) indicate that the distributions are statistically different (null hypothesis is rejected).

Taxon/Group	CC vs. MIX	CC vs. CU	MIX vs. CU
chloro	0.558	0.0109	0.7485
crypto	0.3817	0.0095	0.8791
diat	0.1996	0.0377	0.9878
dino	0.4415	0.019	0.8965
fl	0	0.005	0.0111
hetbact	0	0	0.9098
pelago	0.2032	0.0391	0.988
picoeuk	0.0254	0.9393	0.0095
pro	0.01	0	0.0001
prym	0.4425	0.0192	0.8967
syn	0.0029	0.8109	0.0138
tchl	0.4425	0.0192	0.8967
appen	0.1775	0.9715	0.0989
calanoid	0.0329	0.3312	0.7239
chaeto	0.0268	0.4321	0.5359
cnid	0.0487	0.3800	0.7465
dolio	0.1981	0.2860	0.9906
eggs	0.0401	0.2448	0.8867
euphaus	0.0401	0.2448	0.8867
nauplii	0.0704	0.2077	0.9906
oithona	0.0268	0.2077	0.8692
ostrac	0.8389	0.4818	0.1181
othercop	0.0401	0.2448	0.8867
othercrust	0.0364	0.8228	0.1912
polych	0.0487	0.3800	0.7465
ptero	0.1267	0.0145	0.3025
pyro	NaN	NaN	NaN
rhiz	0.0643	0.0984	0.9576
salp	NaN	NaN	NaN
totvintfl	0.3267	0.4779	0.9953
totvintdiat	0.3267	0.4779	0.9953

Table S3. Same as Table S2 above, but for E-Front Transect E2.

Taxon/Group	CC vs. MIX	CC vs. CU	MIX vs. CU
chloro	0.6601	0.0180	0.3668
crypto	0.4869	0.0140	0.4869
diat	0.1116	0.3402	0.6667
dino	0.7777	0.2227	0.7777
fl	0.0224	0.0050	0.8300
hetbact	0.0841	0.0000	0.4874
pelago	0.6064	0.0510	0.6064
picoeuk	0.9666	0.9662	0.9963
pro	0.1458	0.0000	0.1926
prym	0.9559	0.0680	0.0903
syn	0.6079	0.7643	0.8802
tchl	0.1991	0.0378	0.9559
appen	0.9976	0.7389	0.6575
calanoid	0.1935	0.1193	0.8475
chaeto	0.9710	0.9615	0.8677
cnid	0.9995	0.9827	0.9729
dolio	0.1446	0.0175	0.4306
eggs	0.0940	0.0227	0.6060
euphaus	0.2725	0.4010	0.9998
nauplii	0.1781	0.1394	0.9047
oithona	0.8621	0.7300	0.9365
ostrac	0.9024	0.9326	0.7082
othercop	0.1228	0.0918	0.8868
othercrust	0.2308	0.2327	0.9623
polych	0.7775	0.7389	0.9818
ptero	0.1446	0.0175	0.4306
pyro	NaN	NaN	NaN
rhiz	0.2725	0.0290	0.3621
salp	NaN	NaN	NaN
totvintfl	0.0585	0.0290	0.7810
totvintdiat	0.0585	0.0290	0.7810

Table S4. Description of water-parcel origins for each E-Front transect station based on an ensemble of back-trajectories (100 parcels seeded randomly in a 5-km radius around each station). A water parcel was considered to have originated from the coast (6th column) if its trajectory location was within 25 km of the coastline at any point during the 2-month backtracking. A water parcel was assumed to have been upwelled (last column) if it was at the coast during an upwelling pulse (positive CUTI anomaly). The median age since upwelling and pulse intensity were computed only for upwelled water parcels.

Transect	Station	Median age since upwelling (days)	Median CUTI (m^2/s)	Median CUTI anomaly (m^2/s)	Fraction of parcels from coast	Fraction of upwelled parcels
1	1	51	1.618	0.629	0.68	0.68
1	2	50	2.787	1.727	0.80	0.80
1	3	45	2.130	1.159	0.95	0.95
1	4	45	2.130	1.159	0.91	0.91
1	5	45	2.130	1.159	0.92	0.91
1	6	45	1.020	0.198	0.94	0.94
1	7	32	1.020	0.198	0.95	0.95
1	8	26	1.020	0.198	0.92	0.92
1	9	26	1.020	0.198	0.95	0.95
1	10	26	1.020	0.198	1	1
1	11	26	1.503	0.532	1	1
1	12	15	1.225	0.403	1	0.96
1	13	8	1.248	0.426	1	0.89
2	1	43	0.909	0.222	1	1
2	2	43	0.909	0.222	1	1
2	3	15	1.433	0.612	1	1
2	4	14	1.433	0.612	1	1
2	5	14	1.433	0.612	1	1
2	6	13	1.345	0.524	1	1
2	7	11	0.863	0.042	1	1
2	8	11	0.863	0.042	1	1
2	9	11	0.863	0.042	1	0.91
2	10	11	0.863	0.042	0.96	0.91

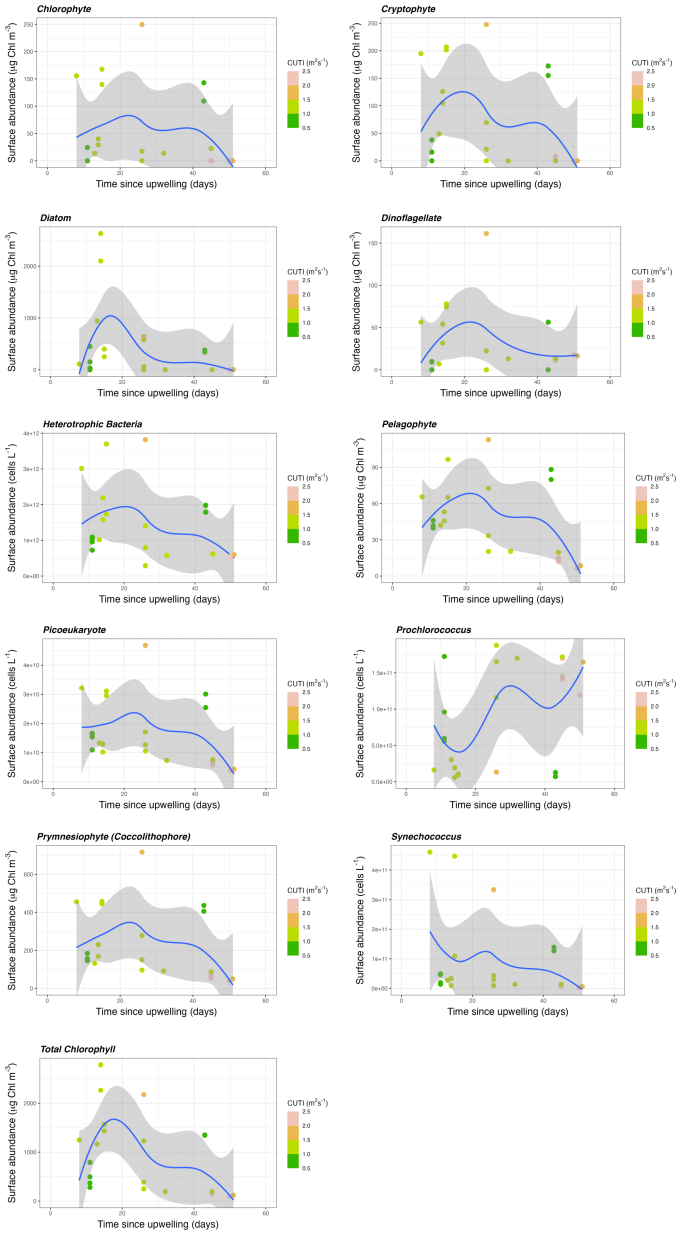

Figure S6. Relationship between phytoplankton and bacteria abundance and age (time) since upwelling, in days. Each marker represents one station; the points include data from both transects. Blue lines represent the lowess fits (f=0.75) of time vs. abundance, with gray shaded regions indicating the 95% confidence interval. The color of the points indicate the median upwelling pulse intensity calculated from the magnitude of CUTI when parcels were at the coast.

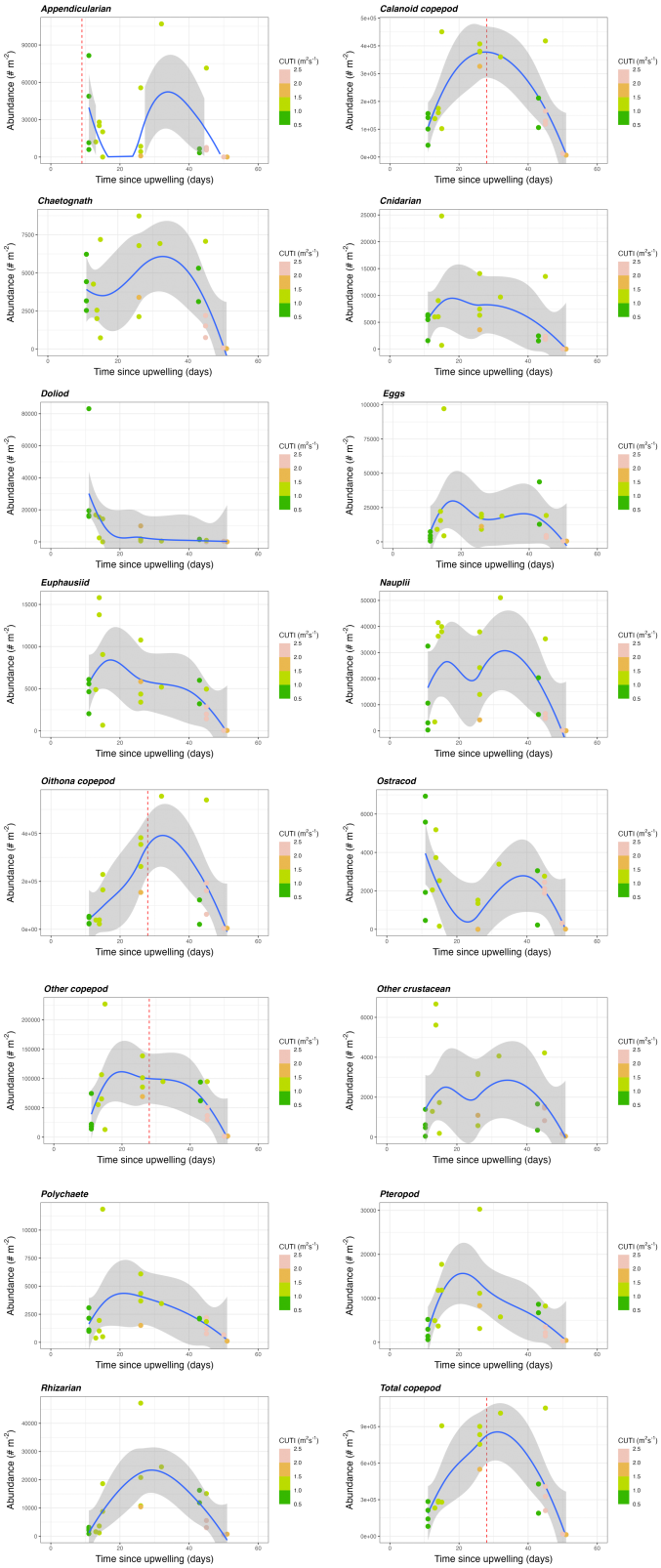

Figure S7. Relationship between zooplankton (and related taxa) abundances and age (time) since upwelling. Each marker represents one station; the points include data from both transects. Blue lines represent the lowess fits (f=0.75) of time vs. abundance, with gray shaded regions indicating the 95% confidence interval. The color of the points indicate the median upwelling pulse intensity calculated from the magnitude of CUTI when parcels were at the coast. Vertical dashed lines in red, when plotted, indicate the estimated generation time of the taxon (e.g., 28 days for copepods).

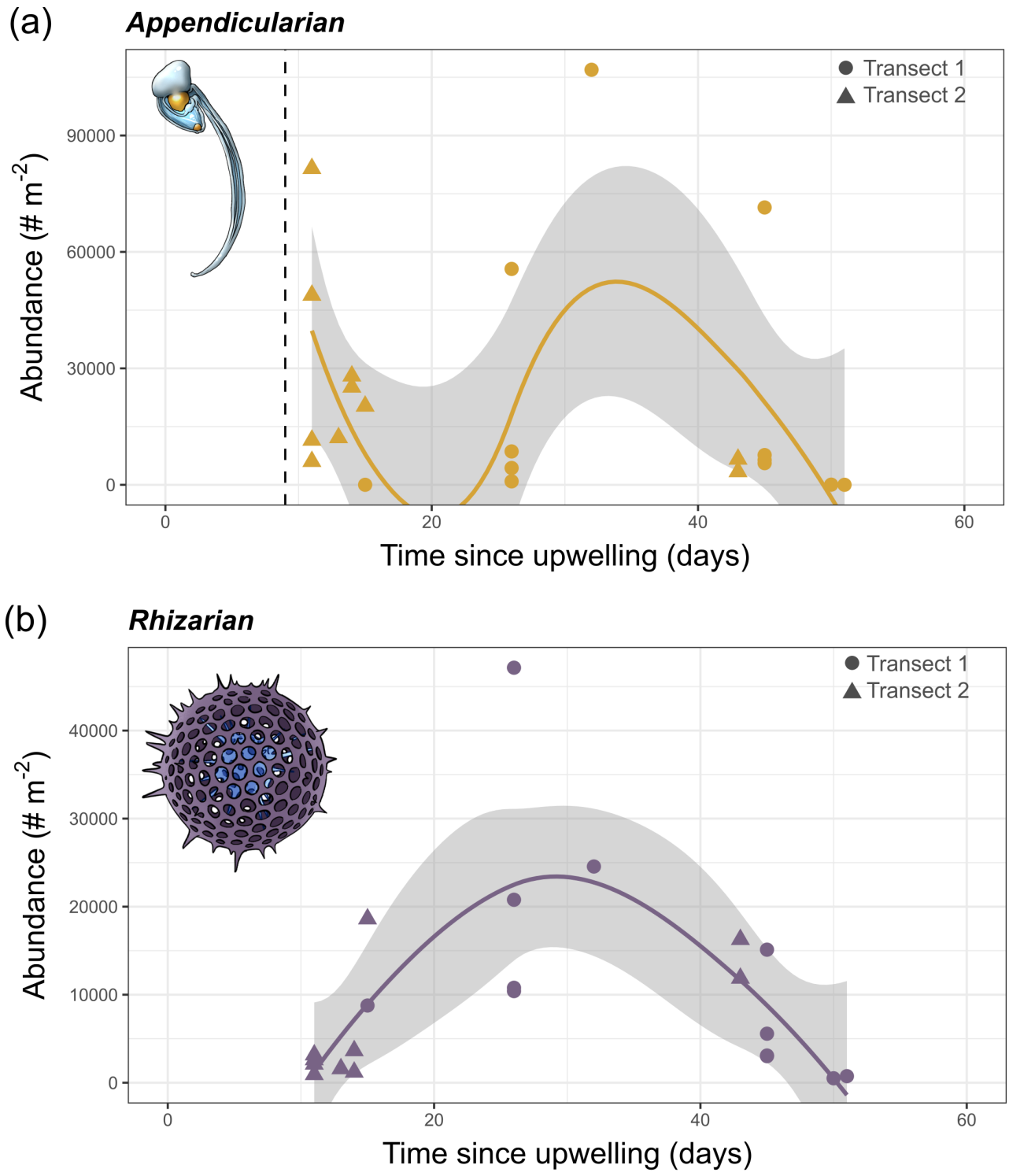

Figure S8. Relationship between plankton abundance and age (time) since upwelling for (a) appendicularians and (b) rhizarians. Each marker represents one station (triangles for Transect E1, circles for Transect E2). The orange and purple lines represent the lowess fits (f=0.75) of time vs. abundance for appendicularians and rhizarians respectively. Gray shaded regions indicate the 95% confidence interval of the lowess fits. The vertical dashed line in (a) shows the typical appendicularian generation time (9 days). Plankton illustrations: Freya Hammar.

References

Biard, M. T. (2015). *Diversité, biogéographie et écologie des Collodaires (Radiolaires) dans l'océan mondial*. PhD thesis.

Biard, T. and Ohman, M. D. (2020). Vertical niche definition of test-bearing protists (Rhizaria) into the twilight zone revealed by in situ imaging. *Limnol. Oceanogr.*, 65(11):2583–2602.

Capitanio, F. L. and Esnal, G. B. (1998). Vertical distribution of maturity stages of Oikopleura dioica (tunicata, appendicularia) in the frontal system off Valdes Peninsula, Argentina. *Bulletin of Marine Science*, 63(3):531–539.

Inomura, K., Karlusich, J. J. P., Dutkiewicz, S., Deutsch, C., Harrison, P. J., and Bowler, C. (2023). High growth rate of diatoms explained by reduced carbon requirement and low energy cost of silica deposition. *Microbiology Spectrum*, 11(3):e03311–22.

Messié, M., Sherlock, R. E., Huffard, C. L., Pennington, J. T., Choy, C. A., Michisaki, R. P., Gomes, K., Chavez, F. P., Robison, B. H., and Smith, K. L. (2023). Coastal upwelling drives ecosystem temporal variability from the surface to the abyssal seafloor. *Proc. Natl. Acad. Sci. U. S. A.*, 120(13):2017.

Whitmore, B. M. and Ohman, M. D. (2021). Zooglider-measured association of zooplankton with the fine-scale vertical prey field. *Limnol. Oceanogr.*, 66(10):3811–3827.